

---

# Correlation of Tumor and Whole-Body Dosimetry with Tumor Response and Toxicity in Refractory Neuroblastoma Treated with $^{131}\text{I}$ -MIBG

Katherine K. Matthay, Colleen Panina, John Huberty, David Price, David V. Glidden, H. Roger Tang, Randall A. Hawkins, Janet Veatch, and Bruce Hasegawa

*Departments of Pediatrics, Radiology, Epidemiology, and Biostatistics, University of California, San Francisco, San Francisco, California*

---

The purpose of our study was to determine the effect of tumor-targeted radiation in neuroblastoma by correlating administered  $^{131}\text{I}$ -metaiodobenzylguanidine (MIBG) activity to tumor and whole-body dosimetry, tumor volume change, overall response, and hematologic toxicity. **Methods:** Eligible patients had MIBG-positive lesions and tumor-free, cryopreserved hematopoietic stem cells. Activity was administered according to body weight and protocol as part of a phase I and phase II study. The whole-body radiation dose was derived from daily 1-m exposure measurements, the tumor self-absorbed radiation dose (TSARD) was determined from scintillation-camera conjugate views, and the tumor volume was measured using CT or MRI. **Results:** Forty-two patients with refractory neuroblastoma (16 with prior hematopoietic stem cell transplant) received a median activity of 555 MBq/kg (15 mCi/kg) (range, 93–770 MBq/kg) and a median total activity of 11,470 MBq (310 mCi) (range, 3,330–30,969 MBq). The median whole-body radiation dose was 228 cGy (range, 57–650 cGy) and the median TSARD was 3,300 cGy (range, 312–30,500 cGy). Responses among evaluable patients included 16 partial response, 3 mixed response, 14 stable disease, and 9 progressive disease. Higher TSARD values predicted better overall disease response ( $P < 0.01$ ). The median decrease in tumor volume was 19%; 18 tumors decreased, 4 remained stable, and 5 increased in size. Correlation was seen between administered activity per kilogram and whole-body dose as well as hematologic toxicity (assessed by blood platelet and neutrophil count nadir) ( $P < 0.05$ ). The median whole-body dose was higher in the 11 patients who required hematopoietic stem cell infusion for prolonged neutropenia versus the 31 patients who did not (323 vs. 217 cGy;  $P = 0.03$ ). **Conclusion:** Despite inaccuracies inherent in dosimetry methods,  $^{131}\text{I}$ -MIBG activity per kilogram correlated with whole-body radiation dose and hematologic toxicity. The TSARD by conjugate planar imaging predicted tumor volume decrease and also correlated with overall tumor response.

**Key Words:** neuroblastoma; MIBG; dosimetry;  $^{131}\text{I}$

**J Nucl Med 2001; 42:1713–1721**

**N**euroblastoma, a childhood tumor derived from the sympathetic nervous system, is the most common extracranial solid tumor of childhood. Although survival for children with advanced disease has improved with the use of intensive multimodality therapy, including autologous bone marrow transplantation, more than half of these children continue to relapse after therapy (1).  $^{131}\text{I}$ -Metaiodobenzylguanidine (MIBG), a guanethidine analog that concentrates in sympathetic nervous tissue (2), provides a means of specific tumor localization for radionuclide delivery to neuroblastoma (3). This agent has a well-established role in detection of primary and metastatic tumor (4) and in eliciting responses in both newly diagnosed (5) and refractory disease (6–9). In phase I and other pilot studies, little toxicity other than myelosuppression has been seen, which can be obviated with autologous hematopoietic stem cell support (8,10,11).

Although multiple attempts have been made to quantify tumor and total-body uptake using the standard conjugate planar imaging method (12), the range of radiation doses delivered to the tumor has varied widely and often has been disappointing when compared with the whole-body radiation dose (13–16). Few reports of dosimetry include correlation of tumor-delivered dose with tumor volume decrease after therapy or correlation of whole-body radiation dose with hematologic toxicity. We report the results of dosimetry calculations based on measurements of whole-body, blood, and tumor activity with correlation with activity administered per kilogram, hematologic toxicity, and tumor volume decrease in patients treated with  $^{131}\text{I}$ -MIBG in a phase I and phase II study for refractory disease.

## MATERIALS AND METHODS

### Patients and Treatment

Patients eligible for this study included any individual  $>1$  y old with refractory or relapsed neuroblastoma whose tumors concentrated  $^{123}\text{I}$ -MIBG or  $^{131}\text{I}$ -MIBG by diagnostic imaging. Patients were required to have a life expectancy of at least 6 wk and a nonpregnant caretaker. At activities of  $\geq 444$  MBq/kg ( $\geq 12$  mCi/

---

Received Dec. 29, 2000; revision accepted Jul. 10, 2001.

For correspondence or reprints contact: Katherine K. Matthay, MD, Department of Pediatrics, Box 0106, University of California School of Medicine, San Francisco, San Francisco, CA 94143-0106.

kg), patients were required to have autologous tumor-free, cryopreserved hematopoietic stem cells available before treatment. Patient characteristics are shown in Table 1. Response and toxicity data on 30 of the 42 patients have been reported with the phase I study (8), but preliminary dosimetry data have been presented for only 5 of the 42 patients included in this study (17). Informed consent was obtained from all patients or the parent or guardian, as appropriate. This study was approved by the University of California Committee on Human Research.

The MIBG was synthesized and exchange-labeled at the University of California, San Francisco (UCSF), by methods described previously (2,8). The specific activity was 1,147–1,369 MBq/mg (10–12 Ci/mmol) with a free iodide content of <5% at the time of administration. All patients were prepared for the <sup>131</sup>I-MIBG treatment with hydration and placement of a urinary catheter for bladder protection. Thyroid-blocking agents (KClO<sub>4</sub> and KI) were given to prevent uptake of radioactive iodine by the thyroid gland as described (8).

The patient was placed on a cardiac and blood pressure monitor for the actual administration. The <sup>131</sup>I-MIBG was infused over 2 h through a dedicated syringe pump. The prescribed activity ranged from 111 to 666 MBq (3–18 mCi) per kilogram for those patients who were part of a phase I <sup>131</sup>I-MIBG activity escalation study or part of an ongoing phase II study at 666 MBq/kg (8). In a few cases, the actual received activity varied from the prescribed activity because of variations in yield. Each patient was kept behind a lead shield until the exposure measurement 1 m from the patient's surface was <2 mR/h (1 R = 2.58 × 10<sup>-4</sup> C/kg). Appropriate radiation safety measures were taken to comply with state and federal guidelines regarding monitoring, waste handling, and personnel exposure.

### Evaluation of Response and Toxicity

Disease evaluation to assess response was done 4–6 wk after treatment and every 3 mo thereafter. Disease evaluation included physical examination, <sup>99m</sup>Tc-methylene diphosphonate bone scan, <sup>123</sup>I- or <sup>131</sup>I-MIBG scan, CT or MRI of gross disease, bone marrow aspirate and biopsy, and measurement of urinary catecholamine metabolites. Precise volumetric measurements were made of an index lesion to monitor quantitative response to <sup>131</sup>I-MIBG. Le-

sions that required palliative external beam radiation were not used in the criteria for response. Complete response denotes no detectable disease by these modalities; partial response indicates a decrease by ≥50% in soft-tissue lesions measured by planimetry from a CT or MR scan and a decrease in nonmeasurable lesions evaluable only by bone scan or MIBG; stable disease indicates no new lesions and no progression in size of a previous lesion by ≥25% for at least 3 mo after therapy; and progressive disease indicates the development of new lesions or increase by >25% in the size of any lesion. Toxicity was monitored by physical examination, complete blood counts, and liver and renal function testing weekly to 4 wk, and then monthly. Endocrine assessment of thyroid and adrenal function was done before treatment, at day 28, then every 3 mo to 1 y, and then yearly. Cardiac function was assessed by echocardiography or multigated radionuclide angiography before and 1 mo after treatment.

### Dosimetry Calculations

The best evaluable tumor (target) lesion was selected on the basis of having detectable <sup>131</sup>I-MIBG uptake and measurable tumor mass. The <sup>131</sup>I-MIBG uptake of the target lesion was measured using conjugate-view planar imaging. More specifically, the scintillation camera was fitted with a high-energy collimator and was peaked for planar imaging of <sup>131</sup>I. A point source consisting of a syringe with a known activity of <sup>131</sup>I was prepared as a calibration source. An anterior planar image of the target lesion and surrounding region was acquired without the point source. The point source was then positioned adjacent to the target lesion, or on the contralateral side, in a position determined visually by a nuclear medicine physician to provide roughly equal attenuation as in the location of the target lesion. The camera was positioned to acquire a posterior planar image of the target lesion and calibration source. The calibration source then was removed to acquire a posterior planar image of the target lesion alone. This produced 4 images: anterior image of the target lesion, anterior image of the target lesion and calibration source, posterior image of the target lesion and calibration source, and posterior image of the target lesion alone.

The image data were processed by placing regions of interest (ROIs) around the target lesion in the anterior and posterior images of the target lesion alone. Background ROIs also are defined adjacent to the target lesion (12) or in a region corresponding to the location of the target lesion on the contralateral side. These values then are used to calculate the geometric mean of background-corrected counts,  $C_t$ , from the anterior ( $C_{t,a}$ ) and posterior ( $C_{t,p}$ ) measurements of the target lesion:

$$C_t = \sqrt{C_{t,a} \cdot C_{t,p}} \quad \text{Eq. 1}$$

Similarly, ROIs were placed around the calibration point source in the anterior and posterior images of the tumor with the point source. Background ROIs for the calibration source were placed in the same location in the images of the tumor alone. These values were used to calculate the geometric mean of background-corrected counts,  $C_s$ , of the anterior ( $C_{s,a}$ ) and posterior ( $C_{s,p}$ ) of the calibration point source:

$$C_s = \sqrt{C_{s,a} \cdot C_{s,p}} \quad \text{Eq. 2}$$

The tumor activity  $A_t$  then was calculated as:

$$A_t = \frac{C_t}{C_s} A_s \quad \text{Eq. 3}$$

**TABLE 1**  
Patient Characteristics

Characteristic	Value*
Median age (y)	6.8 (2–29)
Median time from diagnosis (y)	1.7 (0.5–12)
Prior bone marrow transplantation† (n)	16
Prior chemotherapy (n)	42
Prior radiation (n)	32
Bone metastases (n)	22
Bone marrow metastases (n)	10
Soft-tissue lesions‡ (n)	36

\*Range is in parentheses.

†Four of these patients received 10 Gy of total-body irradiation as part of pretransplant conditioning regimen.

‡Twenty-seven of these patients were evaluable for tumor dosimetry.

n = number of patients.

where  $A_s$  is the known activity of the calibration point source. We note that the calibration point source is imaged after being placed on the patient and that the tumor activity is calculated with a calibration factor equal to the ratio of image counts from the tumor and calibration point source (Eq. 3). Therefore, the conjugate-view method inherently corrects the data for camera sensitivity, attenuation by the body, and dead-time losses, and no additional corrections for these perturbations were performed.

Tumor mass for the index lesion was measured using planimetry from CT or MR scans. The tumor activity measurement described above was performed 2 or 3 times from day 3 to day 7 after treatment and expressed in units of megabecquerels. The tumor activity values then were fit to a single exponential, with tumor dose calculated using the Society of Nuclear Medicine's MIRD schema (18).  $S$  values for self-absorption (i.e., when the target organ is the source organ) for the tumor were calculated from a power-function relationship,

$$\ln S \text{ (Gy/MBq-h)} = -0.967 \ln \text{mass (g)} - 8.634 \quad (r = 0.9965), \quad \text{Eq. 4}$$

obtained using linear regression analysis (i.e.,  $\ln S$  vs.  $\ln \text{mass}$ ) fit to published  $S$  values for organs with masses from 10 g to 70 kg (19). The correlation coefficient ( $r = 0.9965$ ) indicates that the values of  $\ln S$  and  $\ln \text{mass}$  are highly correlated. Furthermore, this relationship can be used to estimate the  $S$  value because, in the case of  $^{131}\text{I}$ , the dose is derived largely from electrons that are absorbed locally, and not from photons. We note that Equation 4 can be used to calculate the dose deposited in the tumor attributed to activity in the tumor, but not from surrounding organs. For this reason, we use the term "tumor self-absorbed radiation dose" (TSARD) to describe the tumor dose calculated using Equation 4.

The whole-body radiation dose was calculated by 2 methods. The first method assumed that the total activity in the whole body is proportional to measurements of radiation exposure rate obtained with an ionization chamber, held in fixed geometry at 1 m from the patient's body surface. In the second method, the whole-body dose was calculated from urine extraction as described below.

The whole-body exposure rate was measured at 1 h after infusion and approximately daily thereafter for 7 d. Five or more data points were obtained for most patients, allowing a double-exponential curve to be fit to the whole-body time-exposure curve. However, when  $<4$  exposure data points were available, the data were fit to a single-exponential curve. In the case of a double-exponential, a time-activity curve having the form

$$A(t) = C_1 \exp(-\lambda_1 t) + C_2 \exp(-\lambda_2 t) \quad \text{Eq. 5}$$

was obtained by nonlinear regression analysis with the software package IGOR (Wavemetrics, Lake Oswego, OR) to determine the exponential time constants ( $\lambda_1$ ,  $\lambda_2$ ) and the coefficients ( $C_1$ ,  $C_2$ ). The coefficients and time constants then were used to obtain the cumulated activity  $\tilde{A}$ :

$$\tilde{A}_{wb} = \int_{t=0}^{\infty} A(t) dt = \frac{A_0}{C_1 + C_2} \left[ \frac{C_1}{\lambda_1} + \frac{C_2}{\lambda_2} \right], \quad \text{Eq. 6}$$

where  $A_0$  is the known activity of  $^{131}\text{I}$ -MIBG injected into the patient at time  $t = 0$ . The whole-body dose was calculated according to the MIRD schema (19) by multiplying the cumulated

activity  $\tilde{A}_{wb}$  by the  $S$  factor for  $^{131}\text{I}$  when the whole body ( $wb$ ) is both the source and the target organ:

$$D_{wb} = \tilde{A}_{wb} S_{wb \leftarrow wb} (^{131}\text{I}). \quad \text{Eq. 7}$$

Similarly, the radiation dose to bone marrow was calculated by multiplying the cumulated activity for the whole body by the  $S$  factor for  $^{131}\text{I}$ , assuming that  $wb$  is the source organ and that bone marrow ( $bm$ ) is the target organ:

$$D_{bm} = \tilde{A}_{wb} S_{bm \leftarrow wb} (^{131}\text{I}). \quad \text{Eq. 8}$$

To calculate doses for children, data files for MIRDOSE (version 2) were used that provide  $S$  values for reference anatomies appropriate for newborns and ages of 1, 5, 10, and 15 y (20). The reference anatomy for 15 y of age also was used for adult women.

The radiation dose  $D_{bl}$  to blood was calculated (21) as the radiation dose to blood attributed to  $\beta$ -particles emitted by radioactivity in the blood ( $\beta$ -component,  $D_{bl,\beta}$ ) added to the radiation dose attributed to  $\gamma$ -radiation arising from radioactivity in the whole body ( $\gamma$ -component,  $D_{bl,\gamma}$ ):

$$D_{bl} = D_{bl,\beta} + D_{bl,\gamma} \quad \text{Eq. 9}$$

To calculate the  $\beta$ -component, blood samples were withdrawn at multiple time points (typically 3, 6, 12, 24, 48, 72, 96, and 168 h after infusion of  $^{131}\text{I}$ -MIBG). The blood samples were allowed to decay to avoid dead-time losses during counting. Known volumes of the blood samples then were withdrawn by pipette and counted in a well counter with a calibration standard to convert measured counts to units of megabecquerels per milliliter. Five or more data points were obtained for most patients, allowing a double-exponential curve to be fit to the blood time-activity curve. However, when  $<4$  exposure data points were available, the data were fit to a single-exponential curve. The cumulated activity  $\tilde{A}_{bl}$  of the blood component was calculated as the integral of the time-activity curve of the blood activity. The  $\beta$ -component then was calculated as:

$$D_{bl,\beta} = \tilde{A}_{bl} \Delta_{\beta} (^{131}\text{I}), \quad \text{Eq. 10}$$

where  $\Delta_{\beta} (^{131}\text{I}) = 1.104 \times 10^{-4} \text{ kg-Gy/MBq/h}$  is the mean energy emitted per unit transition contributed by  $\beta$ -particles from  $^{131}\text{I}$ .

Similarly, the  $\gamma$ -component was calculated as:

$$D_{bl,\gamma} = \alpha [\tilde{A}_{wb} / m_{wb}] \Delta_{\gamma} (^{131}\text{I}), \quad \text{Eq. 11}$$

where  $\tilde{A}_{wb}$  is the cumulated activity of the whole body (in units of MBq-h),  $m_{wb}$  is the mass of the patient, and  $\Delta_{\gamma} (^{131}\text{I}) = 2.175 \times 10^{-4} \text{ kg-Gy/MBq/h}$  is the mean energy emitted per unit transition contributed by  $\gamma$ -rays from  $^{131}\text{I}$ . We note that the values for the mean energy emitted per unit transition were obtained from *MIRD Pamphlet 10* (22) and are similar to values published more recently by Weber et al. (23). In addition, the fraction of the  $\gamma$ -radiation from the whole body that was absorbed by the blood was assigned a value of  $\alpha = 0.4$ , following Benua et al. (21), with the same value of  $\alpha$  used for patients of all ages and sizes.

The whole-body radiation dose measurements were verified by actual comparison with the total activity remaining using the cumulated activity excreted in the urine. For the first 14 treatments, we measured the activity excreted in urine immediately after injection, and at 12, 24, 48, 72, 96, 120, and 148 h after injection, and corrected for physical decay. At each time point, the cumulated (decay corrected) activity excreted in urine was subtracted from the total injected activity to give the total activity remaining

in the whole body without physical decay. These values were multiplied by the appropriate factor to account for physical decay, giving the total whole-body activity remaining in the body, including physical decay. Linear regression analysis of the whole-body dose measurements calculated from urine extraction and from whole-body exposure measurements (Fig. 1) produced a correlation coefficient of  $r = 0.726$  ( $n = 14$ ), corresponding to a significance of  $P < 0.005$  (24), which indicated a close correlation between the results from these 2 methods.

### Statistical Analysis

Data were investigated for correlation between  $^{131}\text{I}$ -MIBG activity administered and tumor volume response, whole-body irradiation dose, and hematologic toxicity, assessed by platelet and neutrophil nadir. Nonparametric or distribution-free statistical tests were chosen to mitigate sensitivity to outlying or influential values (or both). Correlation between continuous variables was summarized with the Spearman rank correlation ( $r_s$ ). Comparisons between unordered data groupings (such as receipt of stem cell infusion) were tested using the Mann-Whitney  $U$  statistics. Comparisons between ordered data groupings (such as tumor response category) used the rank-based trend test of Cuzick (25). Statistical analyses were performed on data from only the first course of treatment to meet the requirement for independent observations and to avoid potential cumulated toxicity effects. All analyses were conducted using STATA 6.0 (StataCorp, College Station, TX).

## RESULTS

### Patients, Response, and Toxicity

Forty-two patients were included in this dosimetry report, including patients treated in the UCSF phase I study (8) and the ongoing phase II study of  $^{131}\text{I}$ -MIBG in refractory neuroblastoma. Of these patients, 32 had soft-tissue lesions, of whom 27 were evaluable for the TSARD. All were evaluable for overall tumor response, for total-body radiation measurements, and for toxicity. All patients were heavily pretreated with prior chemotherapy, most with radiation and

many ( $n = 16$ ) with prior myeloablative therapy with bone marrow support, including 4 who received total-body irradiation (Table 1). The overall response to 1 course of therapy included 16 with partial response, 3 with mixed response, 14 with stable disease for  $>3$  mo, and 9 with progressive disease. All patients treated with  $\geq 555$  MBq/kg (15 mCi/kg) manifested grade 3–4 hematologic toxicity compared with only approximately 50% of those treated at lower doses, as reported in our phase I study (8). Eleven of the patients met criteria for autologous hematopoietic stem cell support after MIBG therapy, including 9 of 17 treated at 666 MBq/kg and 2 of 7 treated at 555 MBq/kg.

### Whole-Body, Blood, and Red Marrow Dose

The median and range for the administered total activity and the activity per kilogram, whole-body radiation dose, blood dose, red marrow dose, tumor dose (TSARD), and tumor volume change are summarized for all evaluable patients in Table 2. The median whole-body dose for patients by level increased progressively with a median dose of 124 cGy at 222 MBq/kg, 159 cGy at 333 MBq/kg, 212 cGy at 444 MBq/kg, and 323 cGy at 555 MBq/kg. The median whole-body dose at 666 MBq/kg was 294 cGy, with more overlap between 555 MBq/kg and 666 MBq/kg (Fig. 2), perhaps associated with the greater variability at this level or the increased number of patients. The Spearman correlation between administered activity per kilogram and whole-body dose received was significant, as shown in Figure 2 ( $r_s = 0.59$ ;  $P < 0.0001$ ). The total activity per kilogram administered also correlated with the whole-body radiation dose ( $r_s = 0.54$ ;  $P < 0.0001$ ). No significant correlation was found between the activity administered per kilogram and the blood dose ( $r_s = 0.18$ ;  $P = 0.4$ ), probably because of the very rapid clearance of MIBG from the blood (26). The red marrow dose correlated closely with the

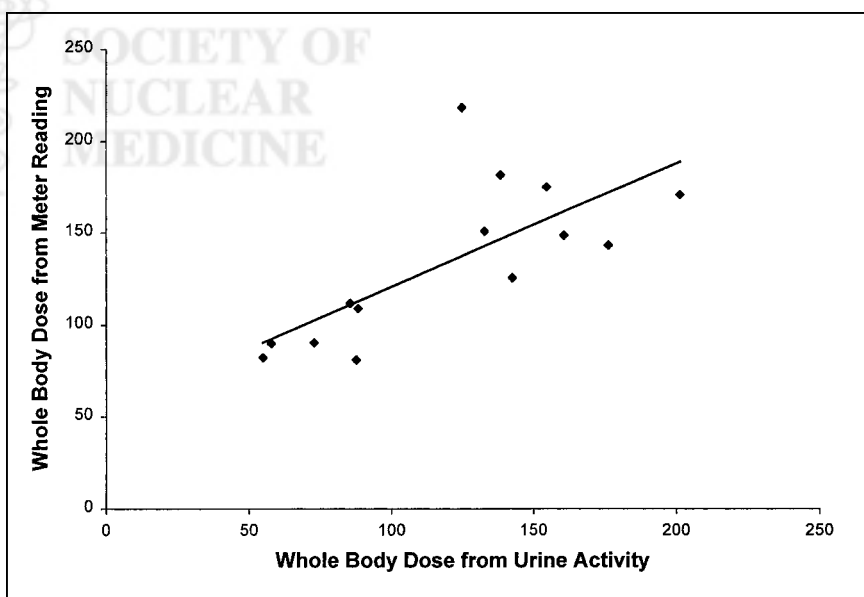


**FIGURE 1.** Comparison of whole-body radiation dose (cGy) calculated from exposure meter readings vs. whole-body dose (cGy) calculated from urine activity.  $P < 0.005$ .

**TABLE 2**  
Summary of Dosimetry Results

Dosimetry parameter	<i>n</i>	Median*	Range*
<sup>131</sup> I-MIBG per kg (MBq)	42	555 (15)	93–770 (2.5–20.8)
Total <sup>131</sup> I-MIBG (MBq)	42	11,470 (310)	3,330–30,969 (90–837)
Whole-body irradiation (cGy)	42	228	57–650
Blood irradiation (cGy)	23	177	79–353
Red marrow irradiation (cGy)	42	220	44–329
TSARD (cGy)	27	3,300	312–30,000
Volume change (%)	26	–19	–100 to +800

\*Millicuries are in parentheses.  
*n* = number of patients.

activity per kilogram ( $r_s = 0.82$ ;  $P < 0.0001$ ), as expected because this is calculated using body weight.

The hematologic toxicities, assessed by the neutrophil and platelet nadir, were significantly associated with increasing activity per kilogram ( $r_s = -0.44$  and  $-0.37$ , respectively) (Table 3) and with the whole-body dose received ( $r_s = -0.56$  and  $-0.40$ , respectively) (Table 3). A significant relationship was found between the activity administered per kilogram and the necessity for stem cell support, with 11 of 24 patients who received  $\geq 555$  MBq/kg of <sup>131</sup>I-MIBG activity requiring stem cell infusion compared with 0 of 18 patients who received  $< 555$  MBq/kg ( $P < 0.001$ ). The median whole-body dose in the 11 patients who required hematopoietic stem cell support for neutropenia was 323 cGy (range, 181–650 cGy) compared with 217 cGy (range, 57–540 cGy) for the 31 patients who did not require stem cell infusion ( $P = 0.03$ ).

**TABLE 3**

Spearman Rank Correlations Among <sup>131</sup>I-MIBG Activity, TSARD, Target Lesion Volume Response, Whole-Body Irradiation Dose, Red Marrow Radiation Dose, and Hematologic Toxicity

Variable (X)	Variable (Y)	$r_s$	<i>P</i>
<sup>131</sup> I-MIBG activity per kg	Whole-body irradiation	0.59	<0.001
	Red marrow irradiation	0.82	<0.0001
	Blood irradiation	0.18	NS
	Neutrophil nadir	–0.44	<0.01
	Platelet nadir	–0.37	0.02
	TSARD	0.32	NS
Total activity of <sup>131</sup> I-MIBG	Volume decrease (%)	0.4	0.04
	Whole-body irradiation	0.57	<0.0001
	Red marrow irradiation	0.49	<0.0001
	Blood irradiation	0.35	NS
	Neutrophil nadir	–0.27	NS
	Platelet nadir	–0.06	NS
Whole-body irradiation dose	TSARD	0.53	<0.01
	Volume decrease (%)	0.29	NS
	Red marrow irradiation	0.61	<0.0001
	Blood irradiation	0.64	<0.0001
	Neutrophil nadir	–0.56	<0.001
	Platelet nadir	–0.4	<0.01
TSARD	TSARD	0.71	<0.0001
	Volume decrease (%)	0.25	NS
	Red marrow irradiation	0.42	0.03
	Blood irradiation	0.51	0.04
	Neutrophil nadir	–0.41	0.04
	Platelet nadir	–0.4	0.04
Red marrow irradiation	Volume decrease (%)	0.47	0.02
	Blood irradiation	0.43	0.04
	Neutrophil nadir	–0.47	<0.01
	Platelet nadir	–0.35	0.02
	Volume decrease (%)	0.48	<0.01

NS = not significant.

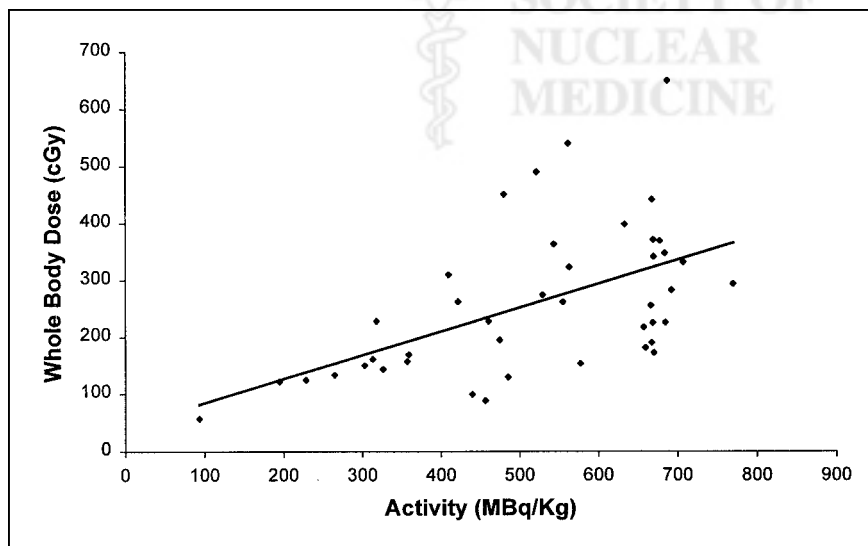


**FIGURE 2.** Correlation of administered activity of <sup>131</sup>I-MIBG per kilogram of body weight with measured whole-body radiation dose. Spearman rank correlation,  $P < 0.0001$ .

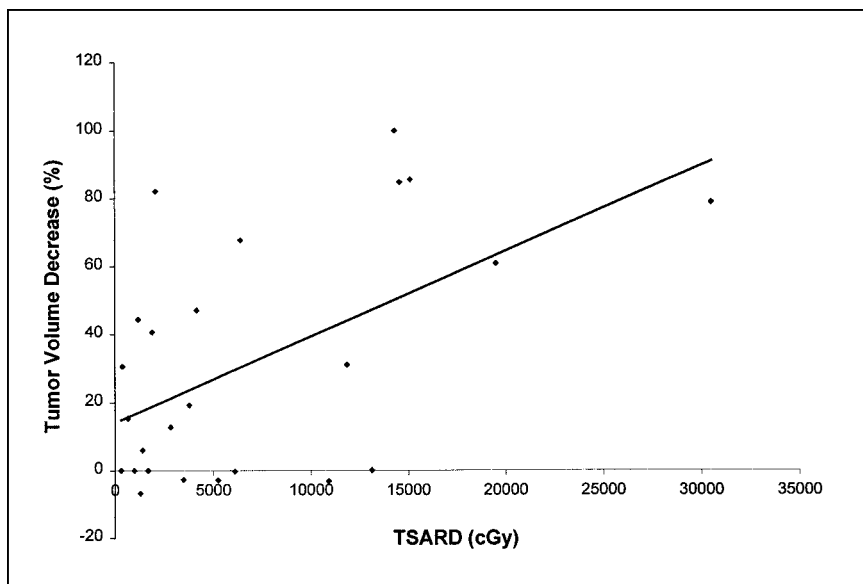


**FIGURE 3.** Correlation of TSARD with subsequent tumor volume decrease. Decrease in tumor volume is shown as positive percentage. Spearman rank correlation,  $P = 0.02$ .

### Tumor Dosimetry, Tumor Response, and Tumor Volume Decrease

Twenty-seven patients were evaluable for the TSARD, and 26 were evaluable for tumor volume decrease. The activity administered per kilogram showed little relationship to the TSARD (Table 3) as one would expect because the TSARD depends on intensity of uptake and the tumor volume distribution. However, a significant correlation was found between the TSARD and the tumor volume decrease (Fig. 3; Table 3). The TSARD also appeared to be a good indicator of overall tumor response, with higher TSARD values predicting better overall tumor response ( $P < 0.01$ ). This is shown in Table 4 by tabulating the tumor response by the tertile of TSARD. The proportion of patients with partial response is much higher in those whose TSARD is  $>7,000$  cGy. Furthermore, progressive disease was seen only in those patients whose tumors received  $<1,700$  cGy. It must also be noted that there were no patients with TSARD values between 7,000 and 10,000 cGy; thus, the highest group actually received an estimated TSARD of  $>10,000$  cGy. The overall partial remission rate of 13 of 27

patients (48%) is slightly higher in the group with evaluable soft-tissue lesions than in the overall group of 16 of 42 (38%).

### DISCUSSION

Two important considerations in MIBG therapy are the nonspecific toxicity and the antitumor efficacy. The ratio of these 2 will determine the overall therapeutic efficacy. The hematologic and possibly the nonhematologic toxicity should be determined by the whole-body radiation dose delivered as well as doses to specific normal organs. However, practically speaking, little nonspecific organ toxicity other than hematologic toxicity has been reported in diverse studies (6,8,27). The main concern, therefore, is prediction and prevention of the hematologic side effects while maximizing tumor delivery of radiation, reflected by the TSARD and the tumor shrinkage.

Ideally, the whole-body dose should correlate accurately with the activity per kilogram. The accuracy of the method of measurement used measuring whole-body retention, also used widely in other studies (13,27), was verified in our study with quantitative urinary excretion of radionuclide. A significant correlation was found between of the whole-body radiation dose and the activity administered per kilogram of body weight. However, there was also interpatient variability, probably attributed, in part, to differing rates of renal excretion (28) and different amounts of body tumor burden and tumor retention. Ways to possibly decrease sources of error include the measurement with a fixed counter rather than a handheld Geiger counter and increasing the number of readings taken per day (29). Pretherapy dosimetry might improve the prediction of total-body dose compared with administering activity based on weight, as has been suggested by others (30). However, it is more tedious, requiring a 5-d pretreatment scan with at least 4

**TABLE 4**

TSARD and Overall Tumor Response in 27 Patients Evaluable for TSARD

TSARD (cGy)	n	Overall disease response			
		PR	MR	SD	PD
$>7,000$	9	7	2	0	0
1,700–7,000	9	3	1	5	0
$<1,700$	9	3	0	3	3

n = number of patients; PR = partial response; MR = mixed response; SD = stable disease; PD = progressive disease.

daily measurements, and still gives significant variability from the posttherapeutic measurements of whole-body dose (27,30). Fielding et al. (29,30) compared the possible error, based on whole-body measurements after treatment, with the activity that would have been prescribed on the basis of either pretherapy dosimetry or body weight. They found that prescribing activity on the basis of body weight would have resulted in the desired whole-body radiation dose ( $\pm 5\%$ ) in 6 patients, too little in 8 patients, and too much in 12 patients, including 5 who would have received an overdose of  $>40\%$ . Using the pretherapy dosimetry, 8 would have received within 5% of the predicted dose, whereas 17 would have been underdosed, and 1 would have been overdosed by 40% (30). In our study, assuming a direct linear relation between activity per kilogram and the whole-body dose received, using the activity prescribed on the basis of body weight resulted in the predicted whole-body dose in 11 patients ( $\pm 10\%$ ), a lower whole-body dose in 18 patients, and a higher-than-expected whole-body dose in 13 patients, including 5 who received a whole-body dose  $>40\%$  higher than expected and 6 who received a whole-body dose  $>40\%$  lower than expected. Given that hematopoietic stem cell infusion has been shown to be effective in the reversal of hematologic toxicity, the increased whole-body radiation dose given in these instances was not serious (no patient received  $>650$  cGy) and may have resulted in greater doses delivered to the tumors because significant correlation was shown between the whole-body dose and the TSARD and between the activity per kilogram and the tumor volume decrease.

We have presented detailed correlation for 42 patients, examining the relationships of activity, activity per kilogram, and whole-body dose to blood, red marrow doses, and myelosuppression, reflected by neutrophil nadir, platelet nadir, and the necessity for hematopoietic stem cell support, using the criterion of an absolute neutrophil count of  $<200$  for  $>2$  wk. The data show that activity administered per kilogram of body weight or the measured whole-body radiation dose correlates significantly with neutrophil nadir and platelet nadir, whereas the total administered activity does not. The blood dose did correlate with the whole-body dose but not with the activity per kilogram, probably because of the proven rapid clearance of activity from the blood, as shown by our data and that of others (17,27,29). Prior studies with smaller numbers of patients have also found some correlation of whole-body dose or activity administered with thrombocytopenia, but they have not explored the relationships over such a broad activity level or tested the correlation with required stem cell support (6,27). We have shown that there is a significant relationship of the activity per kilogram and the whole-body radiation dose to the necessity for stem cell support, with 11 of 24 patients who received  $\geq 555$  MBq/kg of  $^{131}\text{I}$ -MIBG activity requiring stem cell infusion compared with 0 of 18 patients who received  $<555$  MBq/kg ( $P < 0.001$ ). The median whole-body radiation dose for the 11 patients who required hema-

topoietic stem cell support for neutropenia was also significantly higher (323 cGy compared with 217 cGy) than that of the 31 patients who did not require hematopoietic stem cell infusion ( $P = 0.03$ ). Thus, either activity administered per kilogram or estimates of whole-body dose may be used to predict myelosuppression and the likelihood of prolonged neutropenia requiring stem cell support after  $^{131}\text{I}$ -MIBG therapy. Further investigations correlating the effect of tumor burden and the glomerular filtration rate (28) on whole-body dose may be useful.

We have shown with data from a large number of patients that tumor dosimetry is valuable for predicting the volume decrease of the index tumor lesion and the overall disease response. Previous reports of small numbers of children with neuroblastoma found a wide variability in tumor dose delivered and did not express this in relation to activity administered per body weight. This confounded the results for small children compared with larger children or adults, because treatment in most previous studies was at a standard total activity level or whole-body radiation dose (14,29). Previous reports also did not try to verify their calculations by comparisons with disease response or target lesion shrinkage. We found that the volume decrease correlated with the TSARD, thus validating the use of dosimetry despite the variability. Future protocols may further increase the radiation delivered to the tumor by administering 2 successive infusions of  $^{131}\text{I}$ -MIBG with stem cell support to deliver a larger amount of activity in a short time period. Another approach is to find means to enhance MIBG uptake or retention. For example, cisplatin or doxorubicin has been shown to enhance MIBG uptake by neuroblastoma in vitro (31,32) as has increasing expression of the noradrenaline transporter gene, known to be crucial to MIBG uptake (33). Other approaches are to enhance the potency of the radio-labeled MIBG itself, either using no-carrier-added product (34) or using different isotopes with the MIBG, such as  $^{125}\text{I}$  (35,36) or the  $\alpha$ -emitter  $^{211}\text{At}$  (37).

The value of tumor dosimetry has been diminished in the past because of the many sources of error inherent in the conjugate planar method. These include the estimates involved in inhomogeneous uptake within the tumor and difficulties in accurately assessing the tumor volume on CT or MR scans. Although the conjugate-view method uses a calibrated point source to calibrate the data for collimator and detector efficiency, photon attenuation, and scatter radiation, the calibration is obtained at only 1 point and, therefore, does not account for regional variations in the patient. These effects can lead to false-negative interpretations for small lesions or in large patients. Newer techniques of dosimetry that are now under investigation may eliminate some of these problems by fusing the structural CT or MR images with the functional nuclear images to obtain 3-dimensional dosimetry (38,39). Similarly, the development of imaging techniques that combine SPECT with CT, or PET with CT, may improve quantitation of targeted radiodiag-

nostic and radiotherapeutic agents in comparison with methods performed with conventional imaging techniques (40).

## CONCLUSION

Despite inaccuracies inherent in dosimetry methods, <sup>131</sup>I-MIBG activity per kilogram correlated with the whole-body radiation dose, hematologic toxicity, and tumor index lesion volume decrease. The TSARD by conjugate planar imaging predicted the tumor volume decrease and also correlated with the overall disease response. These results suggest that further augmentation of MIBG intensity with hematopoietic stem cell support may improve the response rate by increasing the MIBG activity in the tumor. Tumor and whole-body dosimetry is a valuable means of estimating the therapeutic ratio in radionuclide therapy of tumors.

## ACKNOWLEDGMENTS

The authors thank the nurses of the UCSF Pediatric Clinical Research Center, the nuclear medicine technicians, and the radiation safety personnel for their dedicated work that helped make this study possible. The authors also acknowledge the participation of all of their colleagues in pediatric oncology and nuclear medicine at UCSF—in particular, Drs. Arthur Ablin, Robert Hattner, and Barry Engelstad and Anne Senner, RN, for their help in initiating this study. This work was supported in part by grant 2MO1 RR01271 from the Pediatric Clinical Research Center, by grant 1PO1 CA81403 from the National Institutes of Health, Department of Health and Human Services, and by donations from the Campini Foundation, the Conner Research Fund, and the Kasle and Tkalcevik Neuroblastoma Research Fund.

## REFERENCES

1. Matthay KK, Villablanca JG, Seeger RC, et al. Treatment of high-risk neuroblastoma with intensive chemotherapy, radiotherapy, autologous bone marrow transplantation, and 13-cis-retinoic acid: Children's Cancer Group. *N Engl J Med*. 1999;341:1165–1173.
2. Wieland DM, Wu JL, Brown LE, et al. Radiolabeled adrenergic neuron-labeling agents: adrenomedullary imaging with 131-I-iodobenzylguanidine. *J Nucl Med*. 1980;21:349–353.
3. Hattner RS, Huberty JP, Engelstad BL, et al. Localization of m-iodo (131-I) benzylguanidine in neuroblastoma. *AJR*. 1984;143:373–374.
4. Hadley GP, Rabe E. Scanning with iodine-131 MIBG in children with solid tumors: an initial appraisal. *J Nucl Med*. 1986;27:620–626.
5. Hoefnagel CA, De Kraker J, Valdes Olmos RA, Voute PA. [<sup>131</sup>I]MIBG as a first line treatment in advanced neuroblastoma. *Q J Nucl Med*. 1995;39(4 suppl 1):61–64.
6. Lashford LS, Lewis IJ, Fielding SL, et al. Phase I/II study of iodine 131 metaiodobenzylguanidine in chemoresistant neuroblastoma: a United Kingdom Children's Cancer Study Group investigation. *J Clin Oncol*. 1992;10:1889–1896.
7. Hutchinson RJ, Sisson JC, Shapiro B, et al. 131-I-Metaiodobenzylguanidine treatment in patients with refractory advanced neuroblastoma. *Am J Clin Oncol*. 1992;15:226–232.
8. Matthay KK, DeSantes K, Hasegawa B, et al. Phase I dose escalation of <sup>131</sup>I-metaiodobenzylguanidine with autologous bone marrow support in refractory neuroblastoma. *J Clin Oncol*. 1998;16:229–236.
9. Klingebiel T, Berthold F, Treuner J, et al. Metaiodobenzylguanidine (mIBG) in treatment of 47 patients with neuroblastoma: results of the German Neuroblastoma Trial. *Med Pediatr Oncol*. 1991;19:84–88.
10. Gaze MN, Wheldon TE, O'Donoghue JA, et al. Multi-modality megatherapy with [<sup>131</sup>I]meta-iodobenzylguanidine, high dose melphalan and total body irradiation with bone marrow rescue: feasibility study of a new strategy for advanced neuroblastoma. *Eur J Cancer*. 1995;31A(suppl):252–256.
11. Goldberg SS, DeSantes K, Huberty JP, et al. Engraftment after myeloablative doses of <sup>131</sup>I-metaiodobenzylguanidine followed by autologous bone marrow transplantation for treatment of refractory neuroblastoma. *Med Pediatr Oncol*. 1998;30:339–346.
12. Shulkin BL, Sisson JC, Koral KF, Shapiro B, Want X, Johnson J. Conjugate view gamma camera method for estimating tumor uptake of iodine-131 metaiodobenzylguanidine. *J Nucl Med*. 1988;29:542–548.
13. Flosser JC, Fielding SL. Radiation dosimetry for <sup>131</sup>I-mIBG therapy of neuroblastoma. *Phys Med Biol*. 1996;41:1933–1940.
14. Tristram M, Alaamer AS, Fleming JS, Lewington VJ, Zivanovic MA. Iodine-131-metaiodobenzylguanidine dosimetry in cancer therapy: risk versus benefit. *J Nucl Med*. 1996;37:1058–1063.
15. Bolster AA, Hilditch TE, Wheldon TE, Gaze MN, Barrett A. Dosimetric considerations in <sup>131</sup>I-MIBG therapy for neuroblastoma in children. *Br J Radiol*. 1995;68:481–490.
16. Sisson JC, Hutchinson RJ, Carey JE, et al. Toxicity from treatment of neuroblastoma with <sup>131</sup>I-meta-iodobenzylguanidine. *Eur J Nucl Med*. 1988;14:337–340.
17. Matthay KK, Huberty JP, Hattner RS, et al. Efficacy and safety of [<sup>131</sup>I]metaiodobenzylguanidine therapy for patients with refractory neuroblastoma. *J Nucl Biol Med*. 1991;35:244–247.
18. Loevinger R, Budinger TF, Watson EE. *MIRD Primer for Absorbed Dose Calculations*. New York, NY: Society of Nuclear Medicine; 1989.
19. Snyder WS, Ford MR, Warner GG, Watson SB. "S" *Absorbed Dose per Unit Cumulated Activity for Selected Radionuclides and Organs*. MIRD Pamphlet No. 11. New York, NY: Society of Nuclear Medicine; 1975.
20. Stabin MG. MIRDose: personal computer software for internal dose assessment in nuclear medicine. *J Nucl Med*. 1996;37:538–546.
21. Benua RS, Cicale NR, Sonenberg M, Rawson RW. The relation of radioiodine dosimetry to results and complications in the treatment of metastatic thyroid cancer. *AJR*. 1962;87:171–182.
22. Dillman LT, Von der Lage FC. *Radionuclide Decay Schemes and Nuclear Parameters for Use in Radiation-Dose Estimation*. MIRD Pamphlet No. 10. New York, NY: Society of Nuclear Medicine; 1975.
23. Weber DA, Eckerman KF, Dillman LT, Ryman JC. *MIRD: Radionuclide Data and Decay Schemes*. New York, NY: Society of Nuclear Medicine; 1989.
24. Fisher LD, Van Belle G. *BioStatistics: A Methodology for the Health Sciences*. New York, NY: John Wiley & Sons; 1993.
25. Cuzick J. A Wilcoxon-type test for trend. *Stat Med*. 1985;4:87–90.
26. Lashford LS, Moyes J, Ott R, et al. The biodistribution and pharmacokinetics of meta-iodobenzylguanidine in childhood neuroblastoma. *Eur J Nucl Med*. 1988;13:574–577.
27. Sisson JC, Shapiro B, Hutchinson RJ, et al. Predictors of toxicity in treating patients with neuroblastoma by radiolabeled metaiodobenzylguanidine. *Eur J Nucl Med*. 1994;21:46–52.
28. Wafelman AR, Nortier YL, Rosing H, et al. Renal excretion of meta-iodobenzylguanidine after therapeutic doses in cancer patients and its relation to dose and creatinine clearance. *Nucl Med Commun*. 1995;16:767–772.
29. Fielding SL, Flower MA, Ackery D, Kemshead JT, Lashford LS, Lewis I. Dosimetry of iodine 131 metaiodobenzylguanidine for treatment of resistant neuroblastoma: results of a UK study. *Eur J Nucl Med*. 1991;18:308–316.
30. Fielding SL, Flower MA, Ackery DM, Kemshead J, Lashford LS, Lewis IJ. The treatment of resistant neuroblastoma with <sup>131</sup>I-mIBG: alternative methods of dose prescription. *Radiother Oncol*. 1992;25:73–76.
31. Meco D, Lasorella A, Riccardi A, Servidei T, Mastrangelo R, Riccardi R. Influence of cisplatin and doxorubicin on <sup>125</sup>I-meta-iodobenzylguanidine uptake in human neuroblastoma cell lines. *Eur J Cancer*. 1999;35:1227–1234.
32. Armour A, Cunningham SH, Gaze MN, Wheldon TE, Mairs RJ. The effect of cisplatin pretreatment on the accumulation of MIBG by neuroblastoma cells in vitro. *Br J Cancer*. 1997;75:470–476.
33. Mairs RJ, Livingstone A, Gaze MN, Wheldon TE, Barrett A. Prediction of accumulation of <sup>131</sup>I-labelled meta-iodobenzylguanidine in neuroblastoma cell lines by means of reverse transcription and polymerase chain reaction. *Br J Cancer*. 1994;70:97–101.
34. Mairs RJ, Cunningham SH, Russell J, et al. No-carrier-added iodine-131-MIBG: evaluation of a therapeutic preparation. *J Nucl Med*. 1995;36:1088–1095.
35. Sisson JC, Shapiro B, Hutchinson RJ, Shulkin BL, Zempel S. Survival of patients with neuroblastoma treated with 125-I MIBG. *Am J Clin Oncol*. 1996;19:144–148.
36. Roa WH, Miller GG, McEwan AJ, et al. Targeted radiotherapy of multicell neuroblastoma spheroids with high specific activity [<sup>125</sup>I]meta-iodobenzylguanidine. *Int J Radiat Oncol Biol Phys*. 1998;41:425–432.

37. Cunningham SH, Mairs RJ, Wheldon TE, Welsh PC, Vaidyanathan G, Zalutsky MR. Toxicity to neuroblastoma cells and spheroids of benzylguanidine conjugated to radionuclides with short-range emissions. *Br J Cancer*. 1998;77:2061–2068.
38. Sgouros G, Chiu S, Pentlow KS, et al. Three-dimensional dosimetry for radioimmunotherapy treatment planning. *J Nucl Med*. 1993;34:1595–1601.
39. Koral KF, Zasadny KR, Kessler ML, et al. CT-SPECT fusion plus conjugate views for determining dosimetry in iodine-131-monoclonal antibody therapy of lymphoma patients. *J Nucl Med*. 1994;35:1714–1720.
40. Tang HR, Da Silva AJ, Matthay KK, et al. Neuroblastoma imaging using a combined CT scanner-scintillation camera and <sup>131</sup>I-MIBG. *J Nucl Med*. 2001;42:237–247.

